Cement and Concrete Composites 147 (2024) 105436

Contents lists available at ScienceDirect

Cement and Concrete Composites

journal homepage: www.elsevier.com/locate/cemconcomp

# Toward smart and sustainable cement manufacturing process: Analysis and optimization of cement clinker quality using thermodynamic and data-informed approaches

Jardel P. Gonçalves [a,b], Taihao Han [b,*], Gaurav Sant [c], Narayanan Neithalath [d], Jie Huang [e], Aditya Kumar [b]

[a] Polytechnic School, Federal University of Bahia, Salvador, BA, 40210, Brazil
[b] Department of Materials Science and Engineering, Missouri University of Science and Technology, Rolla, MO, 65409, USA
[c] Department of Civil and Environmental Engineering, University of California, Los Angeles, Los Angeles, CA, 90095, USA
[d] School of Sustainable Engineering and the Built Environment, Arizona State University, Tempe, AZ, 85287, USA
[e] Department of Electrical and Computer Engineering, Missouri University of Science and Technology, Rolla, MO, 65409, USA

ARTICLE INFO

*Keywords:*
Thermodynamic simulation
Cement clinker
Smart manufacturing
High quality clinker
Lime saturation factor

ABSTRACT

Cement manufacturing is widely recognized for its harmful impacts on the natural environment. In recent years, efforts have been made to improve the sustainability of cement manufacturing through the use of renewable energy, the capture of $CO_2$ emissions, and partial replacement of cement with supplementary cementitious materials. To further enhance sustainability, optimizing the cement manufacturing process is essential. This can be achieved through the prediction and optimization of clinker phases in relation to chemical compositions of raw materials and manufacturing conditions. Cement clinkers are produced by heating raw materials in kilns, where both raw material compositions and processing conditions dictate the final chemical makeup of the clinkers. This study uses thermodynamic simulations to analyze phase assemblages of alite- and belite-enriched clinkers based on chemical compositions of raw materials and to create a database. The thermodynamic simulations can accurately reproduce clinker phases in comparison with experimental results. Subsequently, the simulated database is employed to train a data-informed model, and the predictions are used to determine the optimal composition domains that produce high quality clinker ($C_3S$>50 %) at different calcination temperatures. Additionally, optimal lime saturation factor and alumina modulus are investigated to achieve target clinker phases. Overall, this study demonstrates the potential of using a data-informed approach to achieve smart and sustainable cement manufacturing process.

## 1. Introduction

Cement manufacturing is a major contributor to environmental degradation, primarily due to the depletion of natural minerals, the use of fossil fuels, and the emission of significant amounts of $CO_2$. To mitigate these negative impacts, the industry is actively seeking ways to improve manufacturing efficiency, shift toward renewable energy, utilize alternative fuels, and incorporate supplementary cementitious materials. Additionally, the optimization of cement clinker composition is a crucial step toward reducing the environmental impact. Cement plants have used new grinding equipment, dry-process instead of the wet-process kiln, modern clinker kilns, and multi-stage preheaters that can save energy [1]. The use of blends with renewable fuel and fossil fuel [2] or the use of solar calcination reactors [3] can reduce emissions and save energy in cement manufacturing. Furthermore, the use of alternative fuels (e.g., waste tires, waste oil and solvents, sewage sludge, domestic wastes, plastic, textile, and paper wastes) and biomass thermal energy sources (e.g., animal meal, waste wood, sawdust, and sewage sludge) release less greenhouse gas than fossil fuel [4]. By incorporating supplementary cementitious materials (e.g., fly ash and slag) into concrete, a portion of the cement can be replaced, leading to a reduction in environmental impact from alleviating natural resource extraction and $CO_2$ emission [5,6]. Despite the numerous techniques focusing on renewable energy and sustainable cementitious binders, they cannot

* Corresponding author. Department of Materials Science and Engineering, Missouri University of Science and Technology, 140 McNutt Hall, 1400 N Bishop, Rolla, MO, 65409, USA.
*E-mail address:* thy3b@mst.edu (T. Han).

https://doi.org/10.1016/j.cemconcomp.2024.105436
Received 30 March 2023; Received in revised form 6 December 2023; Accepted 5 January 2024
Available online 6 January 2024

fundamentally convert the clinkering process to an efficient and sustainable manner [1,4,7–10]. Modern cement plants strive to achieve maximum thermodynamic efficiency during the manufacturing of cement clinker [8]. To further improve the sustainability of cement production, optimization of the clinkering process is a key factor. This optimization not only leads to improved manufacturing efficiency and reactivity of clinkers, but also delivers substantial benefits, including energy savings, carbon footprint reduction, and natural resource conservation.

Commercially produced cement clinkers can either be alite-enriched (Type I or III Portland cement (PC)) and belite-enriched (Type II or IV PC) [11,12]. Type I or III PC, where $C_3S$ (where: C = CaO; S = $SiO_2$; A = $Al_2O_3$, and F = $Fe_2O_3$) is the dominant phase, is the most prevalent type used in construction. In contrast, belite-enriched cement, where $C_2S$ is the dominant phase, releases less heat and produces small quantities of space-filling reaction products (e.g., calcium-silicate-hydrate) during hydration due to its lower reactivity. Such cements are either used for specific applications or require blending with other types of cement (e.g., PC, calcium sulfoaluminate cement, etc.) to mitigate their negative effects during construction [13,14]. In cement manufacturing, PC with a $C_3S$ content above 50 % is indicative of high-quality clinker. Throughout this manuscript, the term 'cement clinker' generally refers both alite- and belite-enriched clinker, with specific mention made where necessary to distinguish between the two. To evaluate the cement clinker quality, manufacturers typically use the following methods. One type of method is to use the combination of lime saturation factor (LSF), alumina modulus (AM = $Al_2O_3/Fe_2O_3$), silica modulus (SM = $SiO_2/(Al_2O_3+Fe_2O_3)$) [15,16], and the Bogue method [17]. LSF represents the ratio of the amount of lime in the raw material to the theoretical lime required by the major oxides (i.e., $SiO_2$, $Al_2O_3$, and $Fe_2O_3$) (LSF = $100*CaO/(2.8SiO_2+1.18Al_2O_3+0.65Fe_2O_3)$) [15]. For cement clinker, LSF usually ranges from 0.92 to 0.98 [15,16] while AM and SM fall between 1-to-4 and 2-to-3, respectively [15]. LSF can be used to optimize the $C_3S$ in the cement clinker at the clinkering temperature (~1450 °C) [15]. Due to the large variations and combinations in LSF, AM, and SM, manufacturers cannot simply optimize the clinker quality based on these three parameters. The Bogue method then calculates the dominant phases based on the raw material composition [17], but it has limitations (which cannot apply to belite enriched-cement) and may produce inaccurate results, especially for $C_3S$, due to the lack of equilibrium during cooling and the disregard of minor compounds [15,16,18,19].

The abovementioned methods provide only a rough estimation of phase compositions in PC. They are not capable of determining whether the final product will be an alite- or a belite-enriched cement. Therefore, many cement plants determine clinker recipes and assess actual compositions through quantitative x-ray diffraction (XRD) analyses, rather than relying on theoretical calculations. A substantial time difference between testing and manufacturing is expected. Such delayed feedback has made it difficult to implement changes to the manufacturing process, particularly given the potential for causing clinker quality issues. Furthermore, neither XRD analysis nor numerical models can provide information about phase evolution with respect to temperature. In other words, manufacturers are unable to determine the burning zone and the formation of the liquid phase and transitional phases during the heating and cooling processes. Such information can help manufacturers to optimize raw material ratio, enhance clinker quality, and make informed decisions about parameters (e.g., temperature, fuel quantity, etc.) of the clinkering process. Obtaining those details for each new clinker typically requires conducting complex experiments, which can be both costly and technologically challenging. The cement manufacturers require more practical, reliable, and efficient methods to estimate clinker quality when they characterize raw materials.

Thermodynamic simulation is a possible solution, which allows researchers to understand the phase assemblages of cement clinker and influences of raw material composition and calcination temperature. Several studies have demonstrated the capability of using thermodynamic to estimate products of cement clinker. Hokfors et al. [20] synthesized clinkers at 1500 °C to evaluate the formation of a phosphorus belite solid solution and its effect on alite formation. Montoya et al. [21] investigated the effect of iron substitution for aluminum in clinker. Hertel et al. [22] studied synthesizing calcium sulfoaluminate-ferrite clinkers through bauxite residue in combination with other materials. Costa et al. [23] used spend fluid catalytic cracking catalyst to provide additional alumina source during the cement manufacturing. All studies used XRD to analyze phase compositions of clinkers, and subsequently compared the results to thermodynamic simulations. The outcomes from those studies showed that thermodynamic simulations provided better agreement with experimentally-obtained chemical phases compared to the Bogue method, highlighting the utilization of thermodynamic modeling in advancing the understanding of the clinkering process. Thermodynamic simulations can be utilized to predict the phase compositions for clinkers once the raw materials have been known. However, it falls short in performing a reverse engineering task, which means it cannot optimize the blend of the raw materials to achieve target phase compositions of clinkers.

Machine learning (ML) has been widely adopted in the field of cement science to predict the properties of cement as function of their mixture designs. The ML models learn the input-output relationships of cement from a training dataset, and subsequently use this knowledge to predict properties for new cement systems. Such knowledge also can be applied to perform reverse engineering. To be specific, the well-trained ML models can optimize mixture designs of raw materials to achieve target clinker phase compositions. Studies have shown that ML models produce reliable predictions of mechanical properties (e.g., compressive strength [24–26], tensile strength [27,28], and elastic modulus [29–31] of cement. Rheology, which represents the workability of cement systems, is another important property. Artificial neural network [32] and random forest [33] models are employed to predict the rheological properties of fresh cement. Prior research [34–37] showed that ML models capture the trend and produce predictions for the hydration kinetic of sustainable cementitious materials. Additionally, Ali et al. [38] utilized a feedforward network to optimize the clinker manufacturing process by utilizing sensor signals obtained from kilns. ML models can be utilized to improve the quality of clinker and enhance energy efficiency in operating cement plants. The study demonstrates the feasibility of this approach in cement plants with customized infrastructures and limited recipe variations. Notably, our study focuses on predicting the phase compositions of clinkers during heating and cooling processes based on chemical compositions of raw materials. Cement plants can adopt our approach to develop their own recipes, enhance clinker quality, and optimize their manufacturing processes without requiring any infrastructure upgrades. This novel approach distinguishes this study from prior research. In comparison to conventional methods (i.e., experiments and numerical models), ML models have several advantages. ML models do not require x-ray diffraction and X-ray fluorescence analyses, which can be costly. Furthermore, the precision of phase compositions of cement clinkers can also be influenced by the proficiency of researchers in analyzing data. Next, numerical models (e.g., Bogue method) are calibrated for a specific range of compositions and phases. As a result, if the clinker composition falls outside of this range, certain phases may not be able to be calculated. The ML models do not require additional calibration for new cement compositions and can predict all possible phases by knowing simple parameters.

This study employs thermodynamic models to simulate the phase assemblages of cement clinkers (both alite- and belite-enriched cements) during the heating and cooling processes. The thermodynamic model considers influences of temperature and compositions of raw materials on the formation and stability of clinker phases. The reliability of the model is evaluated by comparing its predictions with phase compositions obtained from experiments and bogue method. Additionally, this

study investigates the influences of the LSF and the alumina modulus AM on the phase compositions of cement clinkers. The database obtained from thermodynamic simulations is used to train and validate the performance of a deep learning (DL) model on predicting phase compositions of both alite- and belite-enriched clinkers. To further enhance the manufacturing process, optimal composition domains that produce high quality clinkers ($C_3S$>50 %) are revealed. Moreover, the compositions of raw materials are optimized to achieve target phase compositions of clinkers. To the authors' best knowledge, this is the first study to harness the power of the DL model to enhance the quality of clinkers by optimizing the composition of raw materials and develop a smart manufacturing process.

## 2. Modeling methods

### 2.1. Thermodynamic modeling

This section focuses on analyzing clinkers during heating and cooling processes through thermodynamic modeling, aimed at understanding their phase compositions, developing phase assemblages of the clinkering process, and generating a comprehensive database for the DL model. The research is conducted systematically, following these steps.

In this work, thermodynamic simulations were performed using FactSage free energy minimization software version 8.1 [39]. The simulations used thermodynamic databases for gaseous components (FactPS), and oxides in solid, liquid, and solution phases (FToxid and FTSalt). The performance of thermodynamic modeling was validated by simulating the phase compositions of seven clinkers, obtained from previous studies [15,40–42] (shown in Table 1). For thermodynamic simulations, seven clinkers have been selected from published literature. These clinkers were chosen because of the extensive information provided in these studies, encompassing aspects such as oxide composition, phase composition, and a range of calcination parameters. These parameters span from those used in producing alite-to belite-enriched cements and include data from both industrial and laboratory scales. Clinkers C1 and C2 originate from industrial production, while the others are synthesized in laboratory. The phase compositions of all these cement clinkers except for C1 were measured by quantitative XRD. The phase composition of C1 was obtained from bulk chemical analysis. Each clinker was simulated by heating it to its burning temperature and then cooling it down to 700 °C. All oxide compositions of those clinkers are used as inputs (including major and minor oxides) except for loss of ignition (LOI) in thermodynamic simulations. The computational modeling produced the clinker phase compositions, which were then compared to the experimental results. The calculations were carried out using the equilibrium module and all available products, with a system pressure set at 1 atm.

This study calculated the phase assemblages of clinkers during the heating process between 1000 °C and 1500 °C with 10 °C intervals, and the phase compositions of the cooling process from 1450 °C, 1350 °C, and 1250 °C–700 °C, with 10 °C intervals. The database used in FactSage does not consist of standalone $C_3A$ and $C_4AF$ phases but include the combining phases (e.g., $Ca(Al,Fe)_2O_4$; $Ca_2(Al,Fe)_2O_5$; and $Ca_3(Al,Fe)_2O_6$) [43]. The $Ca_3(Al,Fe)_2O_6$ phase incorporates $C_3A$, while the other phases consist of $C_4AF$. Previous research [20,43,44] indicated the $C_3A$ and $C_4AF$ content as the overall sum of the CaO-$Al_2O_3$-$Fe_2O_3$ solid solutions known as C-A-F. In this study, the $C_3A$ and $C_4AF$ phases are presented together as the $C_3A$+$C_4AF$ phase rather than as C-A-F. Clinkers also comprise minor phases, with the presence of $Na_2O$, MgO, $P_2O_5$, $SO_3$, $K_2O$, $TiO_2$, $Mn_2O_3$, SrO, MnO, ZnO, $V_2O_5$, $Cr_2O_3$, and BaO in the raw materials potentially resulting in numerous minor compounds. Therefore, the outputs of thermodynamic simulations are: $C_2S$; $C_3S$; $C_3A$ + $C_4AF$; CaO; oxide melt (liquid phase), and others. Others represents the sum of all minor phases.

This study performed thermodynamic simulations for new clinkers using the main oxides (i.e., CaO, $SiO_2$, $Al_2O_3$, $Fe_2O_3$, $Na_2O$, and $K_2O$) and a wide temperature range (shown in Table 2) to create a large database to train the DL model. The minor oxides (e.g., MgO, $SO_3$, etc.) are ignored in the simulations for new clinkers. Most $SO_3$ in PC do not engage in the clinkering process; they primarily originate from gypsum, added post-clinkering. Owing to minimal influences on the clinkering process, it is omitted from the database. Moreover. This study represents a pioneering effort in predicting and optimizing the phase composition of cement clinkers using DL model. The primary focus is on evaluating the ability of the model to accurately predict, and eventually optimize, the major phases in cement clinkers. Based on this ability to reliably predict as well as optimize the major clinker phases, future studies will be employed to develop more sophisticated models, which are capable of accounting for the full range of oxide compositions, including exact quantifications of minor phases, in cement clinkers. The database was also analyzed to rigorously evaluate the influences of raw material compositions on major clinker phases. Prior research [45,46] has established that the formation of lime-poor phases such as CS and $C_3S_2$ in cement clinkers occurs when the molar ratio of CaO-to-$SiO_2$ falls between 1 and 1.24. It is noteworthy that these phases are classified as other phases in this study because they do not dissolve in water to participate in the hydration reaction [15].

### 2.2. Deep learning

In this study, a DL [47] model was used to predict phase compositions of cement clinkers during the heating and cooling processes. The DL model consists of multiple computational elements, known as neurons, that are arranged in layers and connected to each other in a way that allows them to process information in a hierarchical fashion. The hierarchical structure is comprised of three main layers: an input layer; one or more hidden layers; and an output layer [48]. The input layer receives information from the dataset and the output layer produces the final outputs to users. The hidden layers are in between the input and output layers, which are responsible for processing the data based on activation and weight functions. The connections between neurons are unidirectional, meaning that information flows in only one direction, from the input layer to the output layer. Additionally, the connections between neurons only exist between consecutive layers, meaning there are no connections between neurons within the same layer or between non-consecutive layers. Each neuron in a DL uses an activation function

**Table 1**
Oxide compositions of the raw materials for seven clinkers and their calcination temperatures obtained from previous studies.

| Sample | CaO | $SiO_2$ | $Al_2O_3$ | $Fe_2O_3$ | $Na_2O$ | MgO | $SO_3$ | $K_2O$ | LOI | Temp. | Ref. |
|---|---|---|---|---|---|---|---|---|---|---|---|
| C1 | 66.40 | 21.90 | 5.70 | 3.20 | 0.20 | 1.20 | 0.40 | 0.50 | 0.60 | 1450 | [15] |
| C2 | 64.81 | 22.44 | 4.67 | 2.59 | 0.41 | 1.36 | 1.01 | 1.26 | 0.66 | 1450 | [40] |
| C3 | 66.56 | 21.25 | 6.34 | 5.23 | 0.13 | 0.07 | 0.01 | 0.27 | 0.14 | 1450 | [41] |
| C4 | 62.81 | 25.00 | 6.34 | 5.23 | 0.13 | 0.07 | 0.01 | 0.27 | 0.14 | 1365 | |
| C5 | 42.38 | 14.64 | 3.68 | 1.62 | 0.12 | 1.41 | 0.05 | 0.71 | 35.39 | 1450 | [42] |
| C6 | 40.36 | 16.85 | 4.23 | 1.85 | 0.14 | 1.58 | 0.06 | 0.82 | 34.11 | 1350 | |
| C7 | 38.27 | 19.12 | 4.79 | 2.1 | 0.16 | 1.75 | 0.06 | 0.93 | 32.82 | 1300 | |

**Table 2**
Chemical compositions and processing conditions of cement clinkers for thermodynamic simulations.

| Composition | CaO | $SiO_2$ | $Al_2O_3$ | $Fe_2O_3$ | $Na_2O$ | $K_2O$ |
|---|---|---|---|---|---|---|
| **Range ($\%_{mass}$)** | 40.0–70.0 | 2.0–54.0 | 3.0–12.0 | 1.0–14.0 | 1.0 | 1.0 |
| **Step size ($\%_{mass}$)** | 5.0 | 100 – other oxides | 3.0 | 1.0, 5.0, 9.0, and 14.0 | | |
| **Heating Temperature** | 1300–1500 | | | | | |
| **Cooling Temperature** | 1500–1300 → 700 °C | | | | | |
| **Temperature Step Size** | 25 °C | | | | | |

to calculate intermediate output values. The activation function takes into account all of the neurons from the previous layer through the weight function and generates a new intermediate output value. This output value is then passed on as input to the next neuron layer. This process continues throughout the network until the final neuron layer is reached, which produces the final output. In this study, the 10-fold cross-validation (CV) method [26,49] and the grid-search method [26,35] are utilized to optimize the number of layers and number of neurons on each layer to avoid overfitting and underfitting. The results shown in this study were conducted by DL with 3 layers and 11 neurons on each layer.

### 2.3. Database collection

The database of cement clinkers was derived from the above-mentioned thermodynamic simulations. The simulations were conducted under heating and cooling processes. In the heating process, precursors were heated to 1300-to-1500 °C, and the chemical phases at high temperatures were outputs. In the cooling process, precursors were cooled from 1300-to-1500 °C to 700 °C, and the chemical phases at 700 °C were outputs. In this study, we utilized a training dataset to train our model and learn input-output correlations. The testing dataset is utilized to evaluate the model's prediction performance. The training dataset consisted of 1008 data-records, and their detailed compositions and processing temperatures are listed in Table 2. The testing dataset included 200 randomly selected data-records, with input variables chosen from within the domain of the training dataset. It is important to note that the training and testing datasets for the heating and cooling processes had identical input parameters. The chemical compositions of raw materials and simulated chemical phases of training and testing datasets are shown in Tables 3 and 4. For both datasets, the input parameters are: CaO content (%); $SiO_2$ content (%); $Al_2O_3$ content (%); $Fe_2O_3$ content (%) and temperature (°C). The $Na_2O$ and $K_2O$ content do not need to be included as input parameters as they remain constant for all data-records. The output parameters are: $C_3S$ content (%); $C_2S$ content (%); CaO content (%); $C_3A + C_4AF$ content (%); oxide melt (%); and other phases (%). This study only focused on chemical phases—the main phases of cement clinkers—that can react with water during the hydration while other inactive phases are considered as other phases. Certain clinkers do not form any $C_3S$ phase, and other formed phases (e.g., $C_2S$, $C_3S_2$, etc.) have lower melting temperature, which leads to 100 % liquid phase at 1500 °C. The prediction accuracy of the DL model on the testing dataset is evaluated by four statistical parameters including: Pearson correlation coefficient ($R$); coefficient of determination ($R^2$); root mean squared error (*RMSE*); and mean absolute error (*MAE*). Equations for the statistical parameters can be found elsewhere [26,50,51].

**Table 3**
Four statistical parameters pertaining the training dataset including 5 inputs and 6 outputs (bold) of 1008 data-records for the heating and cooling processes.

| Attribute | Unit | Min. | Max. | Mean | Std. Dev. |
|---|---|---|---|---|---|
| CaO | % | 40 | 70 | 55 | 10 |
| $SiO_2$ | % | 2 | 54 | 28.25 | 11.59 |
| $Al_2O_3$ | % | 3 | 12 | 7.51 | 3.35 |
| $Fe_2O_3$ | % | 1 | 14 | 7.25 | 4.81 |
| Temperature | °C | 1300 | 1500 | 1400 | 64.54 |
| **Heating** | | | | | |
| **$C_3S$** | % | 0 | 73.51 | 11.52 | 18.70 |
| **CaO** | % | 0 | 41.81 | 4.53 | 9.64 |
| **$C_2S$** | % | 0 | 80.96 | 17.41 | 22.92 |
| **$C_3A + C_4AF$** | % | 0 | 40.26 | 1.89 | 6.18 |
| **Oxide Melt** | % | 17.04 | 100 | 60.85 | 25.42 |
| **Others** | % | 0 | 68.66 | 3.47 | 11.48 |
| **Cooling** | | | | | |
| **$C_3S$** | % | 0 | 87.09 | 13.95 | 20.75 |
| **CaO** | % | 0 | 42.12 | 4.21 | 9.44 |
| **$C_2S$** | % | 0 | 87.09 | 24.48 | 26.62 |
| **$C_3A + C_4AF$** | % | 0 | 48.11 | 14.24 | 14.10 |
| **Oxide Melt** | % | 0 | 41.05 | 2.01 | 5.03 |
| **Others** | % | 6.35 | 100 | 13.31 | 35.22 |

**Table 4**
Four statistical parameters pertaining the testing dataset including 5 inputs and 6 outputs (bold) of 200 data-records for the heating and cooling scenarios.

| Attribute | Unit | Min. | Max. | Mean | Std. Dev. |
|---|---|---|---|---|---|
| CaO | % | 41.15 | 69.94 | 56.35 | 7.91 |
| $SiO_2$ | % | 4.03 | 48.28 | 26.67 | 9.26 |
| $Al_2O_3$ | % | 3 | 12 | 7.56 | 3.35 |
| $Fe_2O_3$ | % | 1 | 14 | 7.41 | 4.53 |
| Temperature | °C | 1300 | 1500 | 1373.37 | 64.13 |
| **Heating** | | | | | |
| **$C_3S$** | % | 0 | 75.87 | 17.91 | 26.18 |
| **CaO** | % | 0 | 35.96 | 1.08 | 5.73 |
| **$C_2S$** | % | 0 | 72.83 | 18.65 | 26.71 |
| **$C_3A + C_4AF$** | % | 0 | 40.26 | 2.57 | 6.71 |
| **Oxide Melt** | % | 17.49 | 100 | 55.81 | 25.19 |
| **Others** | % | 0 | 69.99 | 3.84 | 11.95 |
| **Cooling** | | | | | |
| **$C_3S$** | % | 0 | 76.19 | 17.28 | 24.89 |
| **CaO** | % | 0 | 36.27 | 1.65 | 5.83 |
| **$C_2S$** | % | 0 | 86.21 | 28.54 | 27.58 |
| **$C_3A + C_4AF$** | % | 0 | 48.09 | 16.86 | 13.89 |
| **Oxide Melt** | % | 0 | 13.54 | 1.64 | 3.94 |
| **Others** | % | 8.26 | 100 | 34.01 | 34.14 |

## 3. Results and discussion

### 3.1. Phase assemblages of cement clinker

The thermodynamic simulations were employed to yield the phase assemblages of clinkers (C1-C7) obtained from previous studies. Fig. 1a, b, and c show the phase assemblages of the C1 clinker that was heated to 1500 °C and cooled from 1450, to 1250 °C down to 700 °C. C1 clinker is an example of PC to investigate the influences of temperature on clinker phases. Fig. 1d, and **e** shows the phase assemblages of the C3 clinker that was heated to 1350 °C and cooled from 1350 °C down to 700 °C. C4 clinker is an example of belite-enriched clinker; this clinker has been included to investigate the influence of temperature on clinker phases. Belite-enriched clinker is usually produced at lower temperature compared to PC, and thus, the simulation temperature remains low. The phase assemblages assist researchers to qualitatively and quantitatively understanding the cement clinkering process.

It is important to understand the formation of $C_3S$ in clinker during the heating process, as shown in Fig. 1a. Below 1300 °C, the $C_2S$ is the

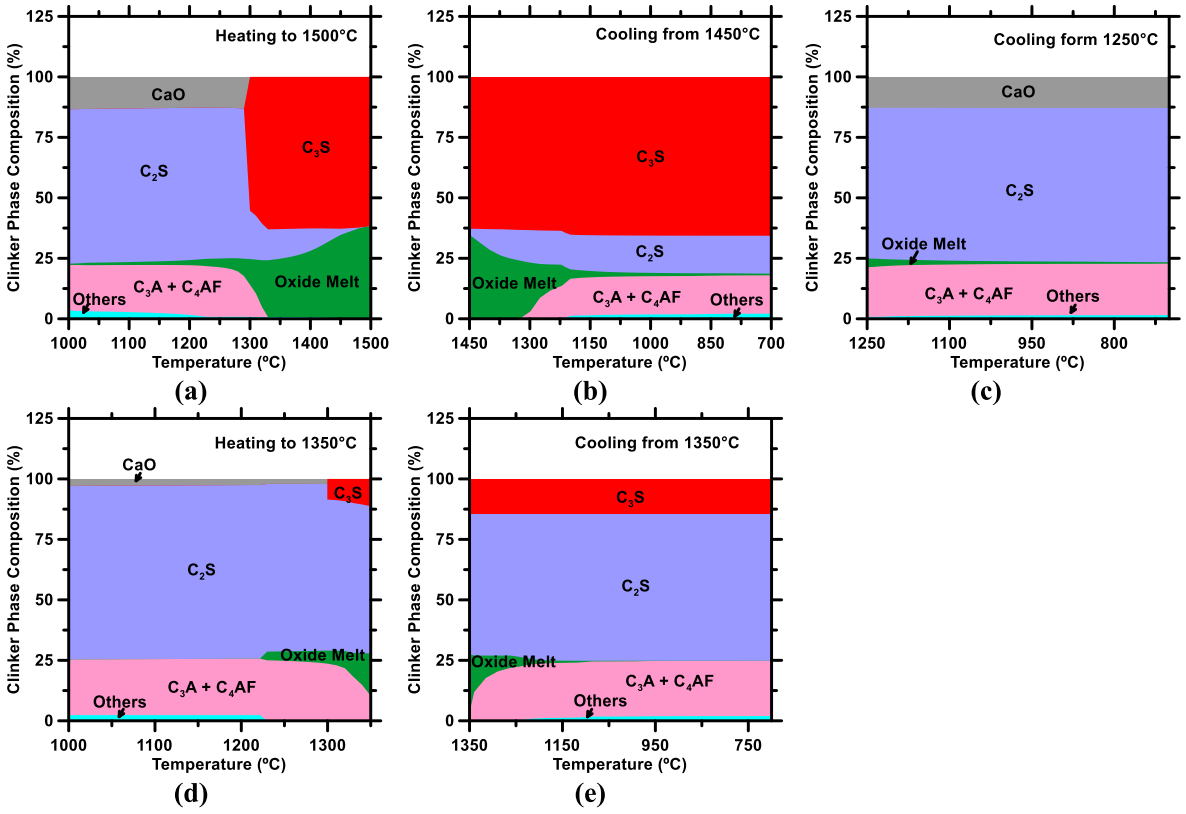


**Fig. 1.** Phase assemblages of C1 clinker obtained from thermodynamic simulations while **(a)** heating to 1500 °C, **(b)** cooling from 1450 to 700 °C, **(c)** cooling from 1250 to 700 °C; and C4 clinker obtained from thermodynamic simulations while **(d)** heating to 1350 °C; and **(e)** cooling from 1350 °C to 700 °C.

dominant phase. Our findings indicate that at around 1300 °C, there is a depletion of CaO and a decrease in the amount of $C_2S$, marked by the initiation of $C_3S$ formation. This finding is in line with previous research [20]. Subsequently, the amount of $C_3S$ remains practically constant up to 1500 °C. The $C_3S$ formation takes place between 1300 and 1450 °C, and the optimal formation of $C_3S$ in the clinker is achieved at 1450 °C [15]. According to Harrisson [16], significant $C_3S$ formation begins near 1450 °C. Hence, to produce cement clinkers with high $C_3S$ content, they must be calcinated 1450 °C, while high $C_2S$ clinker (belite-enriched clinker) must be calcinated below 1300 °C. Up to 1300 °C, the amount of the melting phase remains low, with a concentration below 10.62 %, which corresponds with previous findings in the literature [15]. The minor phases of clinkers contribute to the melting phase. However, as the temperature exceeds 1300 °C, the melting of $C_3A + C_4AF$ phase occurs, resulting in the formation of additional liquid phase and subsequently reducing the system's viscosity. As the temperature surpasses 1350 °C, the $C_2S$—which has not reacted with CaO to form $C_3S$— starts melting and contributes to the formation of additional liquid phase. Those transition temperatures are in agreement with the results reported by Taylor [15]. Strother [16] have argued that the presence of calcium-rich content in the liquid phase can enhance the mobility of $Ca^{2+}$ and accelerate the formation of $C_3S$. Thus, if a clinker contains an adequate amount of $C_3A + C_4AF$ phase, it may require a lower temperature (below 1450 °C) and shorter processing time to complete the formation of $C_3S$.

Fig. 1b demonstrates that $C_3S$ remains in a stable phase during cooling and is not affected by temperature. As the temperature decreases, the liquid phases transform into $C_2S$ and $C_3A + C_4AF$ phases. These three primary phases of clinkers remain unchanged when the temperature reaches 700 °C. The primary reactions during cooling include the crystallization of the melt phase, which produces $C_3A + C_4AF$ phase, and the polymorphic transition of $C_3S$ and $C_2S$ [15]. By comparing the phase assemblages depicted in Fig. 1b and **c,** it becomes evident that the cooling temperature can significantly affect the type and content of the final phases in cement clinkers. At 1250 °C, the insufficient reaction temperature prevents the formation of $C_3S$, resulting in the dominance of $C_2S$, $C_3A + C_4AF$, and CaO. For alite clinker, a high concentration (>5 %) of CaO is undesirable, as excessive CaO can cause unsoundness, as highlighted by Harrisson [16], and potentially compromise the quality of clinkers. The high content of $C_2S$ can influence strength development (belite hydrates more slowly than alite), while high content of $C_3A + C_4AF$ phases can influence rapid set, high evolution of heat, and loss of plasticity in the fresh state [15].

For phase assemblage of belite-enriched cement, as illustrated in Fig. 1d–a relatively small amount of $C_3S$ forms even when heated to 1350 °C. This is in contrast with the scenario depicted in Fig. 1a, wherein an excess of $C_3S$ forms at 1300 °C. The limited formation of $C_3S$ in belite-enriched cement is attributed to a deficiency in free lime, necessary for reacting with $C_2S$. This observation further reinforces the significant impact of chemical composition on the final products of cement clinkers. In the case of belite-enriched cement, belite emerges as the dominant phase, aligning with expectations. Fig. 1e reveals that both $C_2S$ and $C_3S$ maintain stability during cooling and are unaffected by temperature changes. As the temperature decreases, the liquid phases transform into $C_3A$ and $C_4AF$ phases. Owing to the lower processing temperature, $C_2S$ does not transition into a liquid phase. These three primary clinker phases remain unaltered even when the temperature descends to 700 °C. Similar phase assemblage for clinker C4 is also found in the prior study [52].

To evaluate the performance of thermodynamic simulations in reproducing the phases present in cement clinkers, the simulated results are compared with experimental data in Table 5. The comparison is made using a parameter called $I_t$, which represents the difference between the simulated and experimental values. For $C_3S$, $I_t$ ranges from 0.90 to 1.46, while for $C_2S$, $I_t$ ranges from 0.75 to 1.46. For $C_3A + C_4AF$, $I_t$ ranges from 0.94 to 2.21. The typical standard deviation observed in

**Table 5**
Phase assemblages obtained from thermodynamic simulations and deep learning model compared against experimental values.

| Sample | $C_3S$ (%) | $C_2S$ (%) | CaO (%) | Oxide Melt (%) | Others (%) | $C_3A + C_4AF$ (%) | LSF (%) | AM (unitless) |
|---|---|---|---|---|---|---|---|---|
| C1 - 1450 - H | 62.76 | 2.59 | 0 | 34.36 | 0.3 | 0 | 95 | 1.78 |
| C1 - 1450 - C | 65.68 | 15.7 | 0 | 0.66 | 2.1 | 15.85 | | |
| C1-Bogue | 61.29 | 18.18 | – | – | – | 19.91 | | |
| C1 - 1450 - Exp. | 66.9 | 13.2 | 0.6 | 0 | 1.2 | 18 | | |
| $I_b$-C1 | 1.09 | 0.73 | – | – | – | 0.9 | | |
| $I_t$-C1-1450 | 1.02 | 0.84 | – | – | – | 1.14 | | |
| $I_{DL}$-C1-1450 | 1.13 | 0.88 | – | – | – | 1.5 | | |
| C2 - 1450 - H | 62.28 | 3.18 | 0 | 32.09 | 2.45 | 0 | 93 | 1.8 |
| C2 - 1450 - C | 62.36 | 16.97 | 0 | 1.02 | 8.76 | 10.88 | | |
| C2-Bogue | 57.89 | 23.75 | – | – | – | 16.62 | | |
| C2 - 1450 Exp. | 68.6 | 12.8 | 2 | – | – | 24 | | |
| $I_b$-C2 | 1.18 | 0.54 | – | – | – | 1.44 | | |
| $I_t$-C2-1450 | 1.1 | 0.75 | – | – | – | 2.21 | | |
| $I_{DL}$-C2-1450 | 1.1 | 0.81 | – | – | – | 2.77 | | |
| C3 - 1450 - H | 57.62 | 10.11 | 0 | 32.25 | 0.02 | 0 | 95 | 1.21 |
| C3 - 1450 - C | 59.11 | 16.07 | 0 | 0.06 | 2.24 | 22.51 | | |
| C3-Bogue | 59.68 | 16.4 | – | – | – | 24.01 | | |
| C3 - 1450 Exp. | 63.5 | 12.4 | – | – | – | 24.1 | | |
| $I_b$-C3 | 1.06 | 0.73 | – | – | – | 1.01 | | |
| $I_t$-C3-1450 | 1.07 | 0.77 | – | – | – | 1.07 | | |
| $I_{DL}$-C3-1450 | 1.16 | 0.8 | – | – | – | 1.28 | | |
| C4 - 1365 - H | 14.74 | 57.374 | 0 | 26.17 | 0.00 | 1.73 | 78 | 1.21 |
| C4 - 1365 - C | 14.74 | 60.453 | 0 | 0.01 | 1.98 | 22.83 | | |
| C4 - 1365 Exp. | 14.2 | 65.2 | – | – | – | 21.6 | | |
| $I_t$-C4-1365 | 0.96 | 1.08 | – | – | – | 0.94 | | |
| $I_{DL}$-C4-1365 | 0.78 | 1.33 | – | – | – | 1.17 | | |
| C5 - 1450 - H | 60.71 | 0 | 0.25 | 37.94 | 1.1 | 0 | 91 | 2.27 |
| C5 - 1450 - C | 61.28 | 18.55 | 0.25 | 0.01 | 7 | 12.91 | | |
| C5-Bogue | 54.81 | 26.1 | – | – | – | 19.15 | | |
| C5 - 1450 Exp. | 55 | 27 | – | – | – | 18 | | |
| $I_b$-C5 | 1.01 | 1.03 | | | | 0.94 | | |
| $I_t$-C1-1450 | 0.9 | 1.46 | – | – | – | 1.39 | | |
| $I_{DL}$-C1-1450 | 0.91 | 1.57 | – | – | – | 1.86 | | |
| C6 - 1350 - H | 18.08 | 45.19 | 0 | 35.04 | 1.68 | 0 | 76 | 2.29 |
| C6 - 1350 - C | 18.08 | 59.45 | 0 | 0.01 | 7.76 | 14.69 | | |
| C6 - 1350 Exp. | 27 | 56 | – | – | – | 17 | | |
| $I_t$-C1-1350 | 1.49 | 0.94 | – | – | – | 1.16 | | |
| $I_{DL}$-C1-1350 | 1.93 | 0.97 | – | – | – | 1.56 | | |
| C7 - 1300 - H | 0 | 65.08 | 0 | 33.65 | 1.27 | 0 | 63 | 2.28 |
| C7 - 1300 - C | 0 | 72.87 | 0 | 0.03 | 14.48 | 12.62 | | |
| C7 - 1300 Exp. | 0 | 76 | – | – | – | 24 | | |
| $I_t$-C1-1300 | – | 1.04 | – | – | – | 1.9 | | |
| $I_{DL}$-C1-1300 | – | 1.01 | – | – | – | 2.49 | | |

* $I_b$ = experimental value/value from Bogue method; $I_t$ = experimental value/value from thermodynamic simulation at cooling temperature; $I_{DL}$ = experimental value/value from deep learning at cooling temperature.

XRD analysis for determining cement phase composition is ~5 % [53]. On a precursory level, this simulation error range appears to be quite significant. However, a closer examination reveals that most of the results fall within twice the standard deviation of experimental measurements, indicating that the thermodynamic simulations are indeed reliable. When compared to the Bogue method, these thermodynamic simulations demonstrate superior reliability in predicting the phase composition of cement clinker, especially for $C_3S$ and $C_2S$. Furthermore, thermodynamic simulations are capable of accurately determining the phase composition for belite-enriched cement, a feat the Bogue method cannot achieve. The thermodynamic simulations can also predict free lime and minor phases (which are categorized under other phases). The differences between experimental results and thermodynamic simulations can be attributed to a few reasons. First, thermodynamic models cannot account for all processing parameters (e.g., kiln heat uniformity, dwell time, fineness). Therefore, it may not be possible to replicate identical experimental conditions. Second, the database used for thermodynamic simulations does not contain all polymorphic phases, which could potentially lead to slight variations in the results. Finally, measurement errors in the experiments may introduce further differences between the actual and simulated compositions. On the whole, thermodynamic simulations emerge as the most reliable method—at least, in comparison to other competing methods—for revealing the phase composition of all types of cement clinkers, thus reducing or eliminating the need for experiments and XRD analyses. Table 5 presents additional information on LSF and AM of each sample. The data clearly indicates that when the LSF value is greater than 90 %, the dominant phase in the clinker is $C_3S$. On the other hand, if the LSF value is lower than 90 %, there is not enough CaO in the clinker for $C_2S$ to convert into $C_3S$. This results in lower amounts of $C_3S$ and a higher presence of $C_2S$. Furthermore, Table 5 also suggests that a low AM value implies the appearance of more $C_3A + C_4AF$ phases in the clinker. A more detailed study on the influence of LSF and AM on clinker compositions is presented in the next section.

### 3.2. Lime saturation factor and alumina modulus

The previous section demonstrates that thermodynamic simulation is a reliable tool for reproducing the phase assemblages of cement clinker at different processing temperatures. Building on these simulated results, this section examines the impact of LSF on $C_3S$ and $C_2S$ phases across a wide range of cement clinker compositions (shown in Table 2). Fig. 2 shows the $C_3S$ and $C_2S$ phases in clinkers at different LSF levels during both the cooling and heating processes. Notably, more points are observed between 100 % and 150 % LSF during the cooling process than heating. At high temperatures, most $C_2S$ melts and becomes the liquid

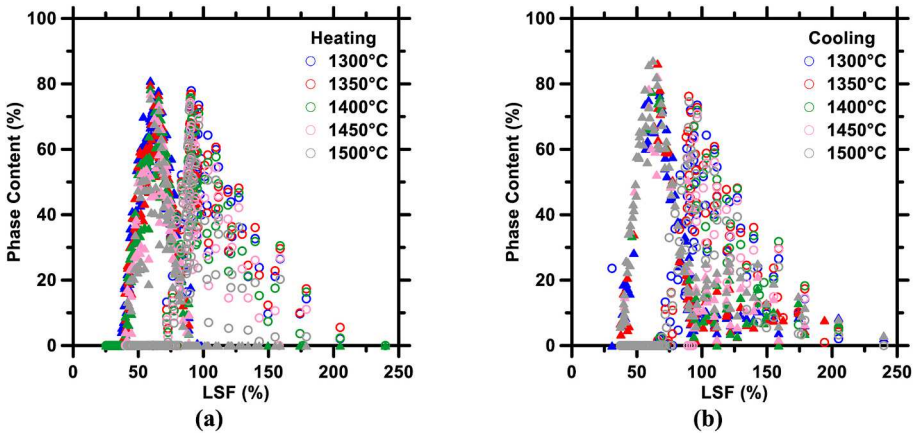


**Fig. 2.** $C_2S$ (solid triangle) and $C_3S$ (hollow circle) content corresponding to LSF at 1300, 1350, 1400, 1450, and 1500 °C as produced by thermodynamic simulations for (a) heating and (b) cooling process. The heating and coolong

phase. Fig. 2 reveals that when LSF is within the range of 59 %–71 %, $C_2S$ is the dominant phase, while LSF in the 89 %–96 % range results in $C_3S$ as the dominant phase. Earlier studies [15,16] have suggested that the ideal LSF range for producing alite is between 92 % and 98 %. However, to date, research has yet to identify the optimal range for belite. LSF is an important factor for cement manufacturing, which can improve the manufacturing process for both alite- and belite-enrich cements.

In the manufacturing of alite-enriched cement, the raw material ratios are adjusted based on LSF because it has been found to be a useful indicator of the clinker composition, especially for $C_3S$. However, there has been a lack of sufficient data supporting the relationship between LSF and $C_3S$, resulting in the adjustment of LSF in a wide range. This wide range of LSF adjustments can lead to inferior raw material ratios that may waste energy and natural minerals in the production of unqualified clinkers. Such clinkers can be detrimental to the overall quality of the final products, resulting in decreased customer satisfaction and increased production costs. To address this issue, this study illustrates a narrow range of LSF required to achieve the optimal $C_3S$ compositions. Manufacturers can use this finding to refine their manufacturing processes, thereby reducing unnecessary waste and promoting product quality.

Belite-enriched cement is a type of low-energy cement that has gained attention due to its potential to reduce energy consumption and $CO_2$ emissions during production [16]. The belite (~1350 kJ/kg) has a lower enthalpy of formation than the main cement phase, alite (~1810 kJ/kg) [54]. In Fig. 1, it is observed that $C_2S$ requires a lower formation temperature than $C_3S$. One method to promote energy reduction and reduce $CO_2$ emissions in cement production is to decrease the LSF of raw materials [55]. This modification increases the belite content and decreases the alite content. However, for belite-enriched clinkers, there have been limited studies on the optimization of the $C_2S$ content with varying LSF. Many studies have shown that the LSF for general cement clinkers ranges from 75 % to 99 % [55–58]. This study indicates the optimal range for belite is 59 %–71 %. It is important to note that belite hydrates more slowly than alite, which can affect the mechanical properties of cementitious materials. Studies [56] have shown that the compressive strength of belite-enriched decreases progressively with increasing LSF values (99, 94, 89, 84, 80, and 75 %) at various ages (1, 3, 19, 30, 100, and 300 days). To address the issue of slower strength development in belite-enriched cement, researchers have suggested improving reactivity or combining it with more reactive cementitious materials (e.g., calcium sulfoaluminate cement). Further research is needed to associate thermodynamic results, reactivity, and mechanical properties in order to optimize the use of belite-enriched cement as a low-energy and sustainable option for the construction industry.

Fig. 3 shows the $C_3A + C_4AF$ phase in clinkers corresponding to different AM levels during both the cooling and heating processes. According to the results shown in Fig. 3, the optimal AM range for $C_3A + C_4AF$ formation is between 0.2 and 3.0, which aligns with prior research reporting typical AM values of 1-to-4 for cement clinkers [15]. Prior literature [13] has indicated that the AM modulus significantly influences the formation of clinker phases, particularly the oxide melt, $C_3A$, $C_4AF$, and the formation temperature of $C_3S$. High AM values signify low $C_3A + C_4AF$ and high viscosity of the clinker system at high temperatures. As aforesaid, sufficient $C_3A + C_4AF$ can enhance the efficiency of $C_2S$ reaction with CaO to form $C_3S$. Consequently, when the AM is around 1, the $C_3A + C_4AF$ can optimally influence the formation of $C_3S$, which can aid in reducing the clinkering temperature and minimizing energy consumption.

### 3.3. Prediction and optimization of clinker quality

In order to produce reliable predictions using the DL model, it is important to meet certain requirements. One key requirement is to have a large enough dataset for the DL model to learn input-output correlations comprehensively. This can be achieved by using a training dataset that contains a sufficient number of data-records, ideally on the order of thousands, and that covers a wide range of domain-specific information. By training on a dataset of this size and diversity, the DL model will be better able to uncover underlying correlations and patterns in the data. Another important requirement for producing reliable predictions is to minimize overfitting and underfitting. Overfitting occurs when a DL model becomes too complex and is able to memorize the training data but is not able to generalize to new data. Underfitting, on the other hand, occurs when the model is too simple to capture the complexity of the data. To minimize these issues, it is important to optimize the hyperparameters of the DL model through techniques such as 10-fold cross-validation and grid-search methods. This will help the model reach its optimal structure and make more accurate predictions on new data. Fig. 4 show predictions of representative phases at heating and cooling processes produced by the DL model compared against results from thermodynamic simulations. The remaining predictions can be found in Fig. S1. Predictions errors evaluated by four statistical parameters are itemized in Table 6.

As shown in Fig. 4 and Table 6, the DL model can produce predictions of chemical phases of cement clinker for heating and cooling processing, with $R^2$ ranging from 0.74 to 0.99, and *MAE* ranging from 0.66 to 7.11 %. The accuracy of predictions for the heating process is higher than those for cooling process. This is due to the fact that in the heating process, a majority of the cement clinker is in the form of melt oxide, making the chemical phases more straightforward and easier to capture.

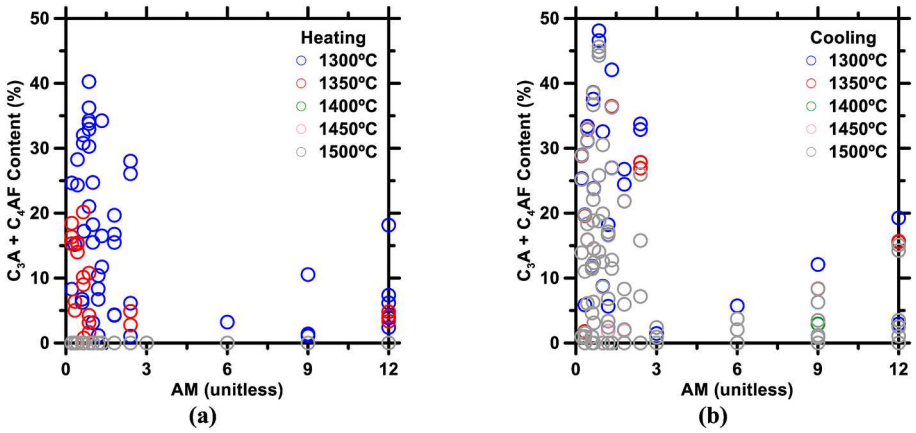


**Fig. 3.** $C_3A + C_4AF$ content corresponding to LSF at 1300, 1350, 1400, 1450, and 1500 °C as produced by thermodynamic simulations for (a) heating and (b) cooling process. Temperature.

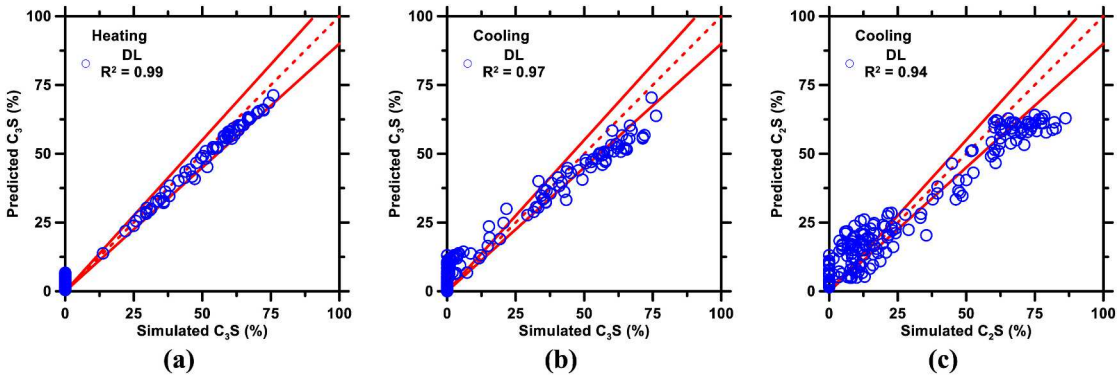


**Fig. 4.** The predictions of representative phases (a) $C_3S$ at heating; (b) $C_3S$ at cooling; and (c) $C_2S$ at cooling of cement clinkers as produced by DL model compared against simulated results. Coefficient of determination ($R^2$) of predictions is shown in legends. The dashed line is ideal prediction, and solid lines represent 10 % errors.

**Table 6**
Statistical parameters evaluating the prediction performance of DL model on chemical phases for heating and cooling scenarios.

| Chemical Phase | R | $R^2$ | MAE | RMSE |
|---|---|---|---|---|
| | Unitless | Unitless | % | % |
| Heating | | | | |
| **$C_3S$** | 0.9978 | 0.9957 | 2.881 | 3.346 |
| **$C_2S$** | 0.9959 | 0.9919 | 3.111 | 3.586 |
| **CaO** | 0.9952 | 0.9905 | 1.071 | 1.194 |
| **$C_3A + C_4AF$** | 0.9740 | 0.9489 | 0.959 | 1.606 |
| **Oxide Melt** | 0.9927 | 0.9855 | 2.922 | 3.635 |
| **Others** | 0.9678 | 0.9367 | 2.463 | 3.449 |
| **Cooling** | | | | |
| **$C_3S$** | 0.9851 | 0.9705 | 4.743 | 6.171 |
| **$C_2S$** | 0.9704 | 0.9416 | 7.118 | 8.806 |
| **CaO** | 0.9931 | 0.9861 | 0.684 | 0.874 |
| **$C_3A + C_4AF$** | 0.9881 | 0.9765 | 1.528 | 2.143 |
| **Oxide Melt** | 0.8603 | 0.7401 | 1.090 | 1.935 |
| **Others** | 0.9879 | 0.9759 | 4.574 | 5.586 |

In contrast, in the cooling process, the melt oxide forms various chemical phases, leading to a more complex database and a decrease in prediction accuracy. Generally, the DL model predicting the chemical phases of cement clinkers in a high-fidelity is made possible by the employment of a series of nonlinear logistic-transfer functions as activation functions for the neurons. These functions allow the model to develop complex input-output correlations, making it suitable for this task. During training, DL models utilize a local search-and-optimization mechanism [59–61] to find the optimal hyperparameters that minimize the error between the predicted and actual outputs. This approach generally leads to faster convergence and more reliable detection of extrema in the dataset. However, one of the main disadvantages of DL model is that it may converge to a local minimum rather than the global minimum, which can lead to inaccurate predictions. While this drawback is often inconsequential in datasets with broadly linear and/or monotonic input-output relationships, it can potentially lead to inaccurate predictions in the case of cement clinker, as the input-output correlations are expected to be complex and highly nonlinear. In this study, we addressed this issue by rigorously optimizing the hyper-parameters of the models through the 10-fold CV and grid search method [36,62]. It is expected that this optimization will overcome the inherent drawbacks of the DL model, allowing it to produce predictions in a high-fidelity manner.

After predicting cement clinker phases obtained from thermodynamic simulation, the DL model is employed to predict the phase composition of real cement clinkers (shown in Table 1). The predictions are compared with measured values and evaluated using $I_{DL}$ (shown in Table 5). The results indicate that the DL model performs less accurately compared to thermodynamic simulations. This is because the model is developed based on data from these simulations, which may have discrepancies with real values. When the DL model produces predictions, it also introduces some errors to predictions. Due to the accumulation of errors, the DL model predicts phase compositions for real cement clinkers with moderate accuracy. To improve the accuracy, the model should be trained using a large and diverse database consisting solely of experimental data.

To further investigate the application of DL models in enhancing smart manufacturing processes, we conducted an extensive study to identify the optimal domains for producing high-quality clinkers ($C_3S$>50 %) at different calcination temperatures, which involves predictions for various combinations of components in clinkers. As illustrated in Fig. 5, the optimal composition domain for high-quality clinkers is situated within the temperature range of 1300-1500 °C; and the composition domain [63] used by manufacturers is also shown. At 1300 °C, a minimal optimal composition domain is observed, which is primarily due to the insufficient activation energy provided at this temperature to trigger the reaction that forms $C_3S$ from most $C_2S$. When the molar ratio of CaO-to-$SiO_2$ exceeds 3, $C_2S$ is more inclined to integrate additional Ca atoms (occurring at the crystallization of $C_3S$) due to the excess amount of free CaO. As the temperature increases to 1350 and 1400 °C, a slight expansion of the optimal domain is noticed, though it still necessitates a CaO-to-$SiO_2$ molar ratio greater than 3 but provides more availability in compositions. According to various studies [15,43,44], the majority of alite formation occurs after 1450 °C. Consequently, a substantial optimal domain region for high-quality clinkers emerges at 1450 and 1500 °C. When the CaO-to-$SiO_2$ molar ratio is higher than 1.6, $C_3S$ content can surpass 50 % at elevated temperatures. Compared to the prevailing optimal domain used by manufacturers, the domain identified in our study offers increased flexibility in terms of composition for producing superior quality clinkers. Moreover, when comparing the domains at 1450 and 1500 °C, it is evident that increasing the temperature does not significantly enhance $C_3S$ formation. As a result, it is not necessary to calcinate the clinker above 1450 °C during the manufacturing process.

The abovementioned results demonstrate that a well-trained deep learning model, with optimized hyperparameters, can predict the phase compositions of cement clinkers under various heating and cooling conditions in a high-fidelity manner. The model's ability that uncovers the underlying relationships between the composition of raw materials and clinker phases can be utilized to optimize raw material ratios that achieve target phase compositions. To verify this hypothesis, the DL model in connection with a Bayesian optimization module [31,50,62,64,65] is utilized to optimize raw material ratios of clinkers that satisfy target $C_3S$ content. In the optimization process, the target $C_3S$ content was set to a range of 0–70 % with 5 % step size. Two types of clinkers were selected: (1) 6 % $Al_2O_3$ and 9 % $Fe_2O_3$, cooled from 1400 °C; and (2) 9 % $Al_2O_3$ and 6 % $Fe_2O_3$, cooled from 1450 °C. The deep learning model was then utilized to determine the optimal contents of $SiO_2$ and CaO that would achieve the target $C_3S$ content. The optimization results are presented in Fig. 6. To provide a comparison, the oxide compositions obtained from thermodynamic simulations are also included in the figure.

The results of the DL model, as shown in Fig. 6, are in good agreement with the data obtained from thermodynamic simulations. This agreement between the predictions and experimental data provides confidence in the DL optimization. The data in Fig. 6 also reveals a counterintuitive trend. As the $C_3S$ content increases, the CaO-to-$SiO_2$ ratio shows an initial rise and then drops when the $C_3S$ content surpasses 30 %. This raises an issue where a single composition may correspond to two different $C_3S$ content, which is incorrect in real experiments. This is also the reason that the downward part in Fig. 6a does not agree with outcomes of thermodynamic simulations. We hypothesize that additional constraints could be applied to the optimization process to avoid this issue; this strategy, which is admittedly nontrivial, will be explored in future studies aimed at modeling and predicting both minor and major phases of cement clinkers. Clinkers with high $Al_2O_3$ and $Fe_2O_3$ content consume a significant amount of CaO to form $C_3A$ + $C_4AF$ phases, leading to clinkers with low $C_3S$ content, and vice versa. The correlation between $Al_2O_3$-$Fe_2O_3$ and $C_3S$ has not been thoroughly studied in both previous and current studies, so constraints have not been applied. Overall, the optimization results suggest that the DL model can effectively optimize raw material ratios of clinkers, which meets the desired phase compositions. This capability is significant, as it enables the DL model to quickly and accurately determine the ideal raw material

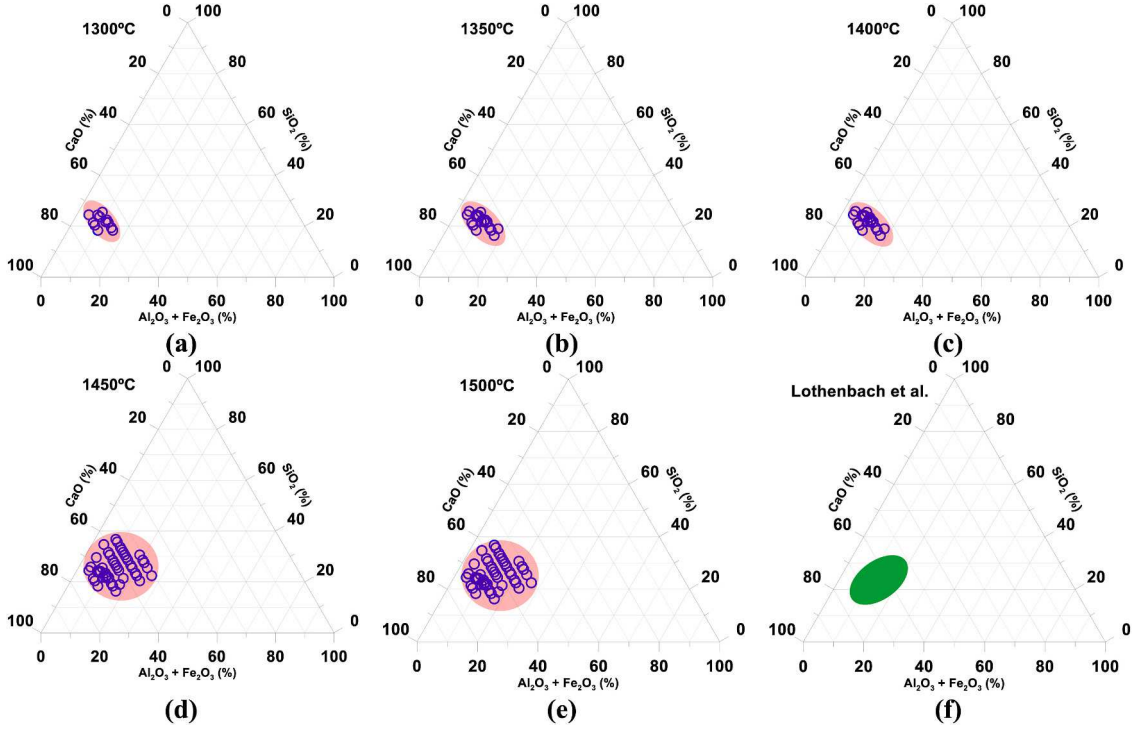


**Fig. 5.** The optimal composition domain of high quality cement clinkers ($C_3S$ > 50 %) at **(a)** 1300 °C; **(b)** 1350 °C; **(c)** 1400 °C; **(d)** 1450 °C; and **(e)** 1500 °C. According to Lothenbach et al. [63], the manufacturers' current optimal clinker domain is represented by **(f)**. The optimal region is highlighted in color, and representative compositions within this domain are denoted by blue circles. (For interpretation of the references to color in this figure legend, the reader is referred to the Web version of this article.)

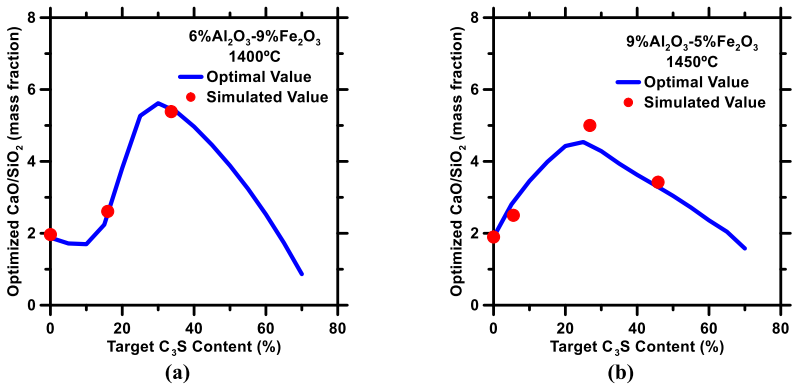


**Fig. 6.** The optimized CaO and $SiO_2$ content as produced by DL model to achieve target $C_3S$ content in cement clinkers. The clinkers are composed of (a) 6 % $Al_2O_3$ and 9 % $Fe_2O_3$, and are cooled from 1400 °C; and (b) 9 % $Al_2O_3$ and 6 % $Fe_2O_3$, and are cooled from 1450 °C. The target $C_3S$ content is indicated by x-axis, and optimal composition is show by y-axis. The blue line represents the optimized compositions and red dots represents actual composition obtained from thermodynamic simulations. (For interpretation of the references to color in this figure legend, the reader is referred to the Web version of this article.)

ratios, even in cases where the underlying cause-effect correlations are not completely understood. By training the DL model with comprehensive databases, it has the potential to optimize raw material ratios of clinkers, which not only satisfy target phase compositions but also performance and sustainability criteria.

## 4. Conclusions

Cement manufacturing has harmful effects on the natural environment, which releases large amounts of $CO_2$ and other greenhouse gases. To enhance the sustainability of cement industry, it is essential to optimize the manufacturing process. This involves predicting and optimizing the major clinker phases in relation to the chemical composition of raw materials and manufacturing conditions. The chemical compositions of raw materials play a significant role in determining the phase composition of final clinkers. Manufacturers must carefully select and mix the raw materials to achieve the desired phase compositions. Manufacturing conditions such as the temperature and duration of heating and cooling also affect the phase compositions of final products. The optimization process involves adjusting these manufacturing conditions to achieve the desired phase compositions with the minimum amount of energy consumption. This study employed thermodynamic simulations to calculate the phase compositions of cement clinkers during the heating and cooling processes based on the oxide compositions of the raw materials. The effects of LSF and AM on the phase compositions of clinkers were investigated. Additionally, the DL model was employed to predict the phase compositions of clinkers and determine the optimal composition domains that produce high quality clinkers at various calcination temperature.

The thermodynamic model provided valuable insights into the formation and phase transition of clinkers during the heating and cooling processes, including $C_2S$, $C_3S$, $C_3A + C_4AF$, and oxide melt. At around 1300 °C, CaO reacted with $C_2S$ to form $C_3S$ during the heating process. No significant final product changes were observed while cooling from 1350 to 1500 °C. Cooling the clinker from 1250 °C resulted in the appearance of CaO and high $C_3A + C_4AF$ content but did not allow $C_3S$ formation. The optimal LSF range for producing alite- and belite-enriched clinkers was around 59–71 % and 89–96 %, respectively. The DL model yielded reliable predictions of cement clinker phase compositions obtained from thermodynamic simulations. The outcomes also assist to determine the optimal composition domains that form high $C_3S$ content at different temperature. When the molar ratio of CaO-to-$SiO_2$ exceeds 3, the clinker can form sufficient $C_3S$ at 1300 °C. When the ratio reduces to 1.6, 1450 °C is required to calcinated high quality clinkers. Moreover, the DL model showed the capability to optimize the compositions of raw materials to achieve target $C_3S$ phases. This study demonstrates the potential of using the DL model to assist cement manufacturers in producing high-quality cement clinkers. However, there are several areas where future research could yield further improvements. One possibility is the development of a high-temperature thermodynamic simulation methodology that is more reliable and cost-effective than current thermodynamic simulations, which would enhance the quality of the database used to train the DL model. Additionally, incorporating minor oxides into the DL model could significantly improve its predictive accuracy and generalizability. Furthermore, implementing additional constraints (e.g., thermodynamic constraints) within the optimization process will help in preventing the suggestion of unrealistic raw material compositions.

Overall, the combination of thermodynamic simulation and machine learning models can be a promising tool for the development of new recipes and optimization of the clinkering processes, leading to a smart manufacturing process. By using these tools to guide the selection of raw materials, process parameters, and production pathways, it is possible to produce sustainable clinkers that meet high-quality standards. This can help reduce the environmental impact of cement production while maintaining the economic viability of the industry.

## CRediT authorship contribution statement

**Jardel P. Gonçalves:** Conceptualization, Funding acquisition, Investigation, Writing – original draft. **Taihao Han:** Formal analysis, Investigation, Software, Writing – original draft. **Gaurav Sant:** Funding acquisition, Supervision, Writing – review & editing. **Narayanan Neithalath:** Funding acquisition, Supervision, Writing – review & editing. **Jie Huang:** Funding acquisition, Writing – review & editing, Supervision. **Aditya Kumar:** Conceptualization, Funding acquisition, Supervision, Writing – review & editing.

## Declaration of competing interest

The authors declare that they have no known competing financial interests or personal relationships that could have appeared to influence the work reported in this paper.

## Data availability

Data will be made available on request.

## Acknowledgments

This study is financially supported by the Improvement of Higher Education Personnel (CAPES - *Coordenação de Aperfeiçoamento de Pessoal*

*de Nível Superior* - Grant number 88887.694501/2022–00); National Science Foundation (NSF-DMR: 2228782); and the Kummer Institute (Missouri S&T) Ignition Grant. Thanks Dr. Ana R. D. Costa for providing two thermodynamic simulation results in this study.

## Appendix A. Supplementary data

Supplementary data to this article can be found online at https://doi.org/10.1016/j.cemconcomp.2024.105436.

## References

[1] D. Coffetti, E. Crotti, G. Gazzaniga, M. Carrara, T. Pastore, L. Coppola, Pathways towards sustainable concrete, Cement Concr. Res. 154 (2022) 106718, https://doi.org/10.1016/j.cemconres.2022.106718.
[2] A. Tsiligiannis, C. Tsiliyannis, Renewable energy in cement manufacturing: a quantitative assessment of energy and environmental efficiency of food residue biofuels, Renew. Sustain. Energy Rev. 107 (2019) 568–586, https://doi.org/10.1016/j.rser.2019.03.009.
[3] G. Moumin, M. Ryssel, L. Zhao, P. Markewitz, C. Sattler, M. Robinius, D. Stolten, $CO_2$ emission reduction in the cement industry by using a solar calciner, Renew. Energy 145 (2020) 1578–1596, https://doi.org/10.1016/j.renene.2019.07.045.
[4] S. Supino, O. Malandrino, M. Testa, D. Sica, Sustainability in the EU cement industry: the Italian and German experiences, J. Clean. Prod. 112 (2016) 430–442, https://doi.org/10.1016/j.jclepro.2015.09.022.
[5] T. Hemalatha, A. Ramaswamy, A review on fly ash characteristics – towards promoting high volume utilization in developing sustainable concrete, J. Clean. Prod. 147 (2017) 546–559, https://doi.org/10.1016/j.jclepro.2017.01.114.
[6] C.-M. Aldea, F. Young, K. Wang, S.P. Shah, Effects of curing conditions on properties of concrete using slag replacement, Cement Concr. Res. 30 (2000) 465–472, https://doi.org/10.1016/S0008-8846(00)00200-3.
[7] K. Scrivener, F. Martirena, S. Bishnoi, S. Maity, Calcined clay limestone cements (LC3), Cement Concr. Res. 114 (2018) 49–56, https://doi.org/10.1016/j.cemconres.2017.08.017.
[8] M. Sharma, S. Bishnoi, F. Martirena, K. Scrivener, Limestone calcined clay cement and concrete: a state-of-the-art review, Cement Concr. Res. 149 (2021) 106564, https://doi.org/10.1016/j.cemconres.2021.106564.
[9] R. Snellings, Assessing, understanding and unlocking supplementary cementitious materials, RILEM Technical Letters 1 (2016) 50–55, https://doi.org/10.21809/rilemtechlett.2016.12.
[10] H.-M. Ludwig, W. Zhang, Research review of cement clinker chemistry, Cement Concr. Res. 78 (2015) 24–37, https://doi.org/10.1016/j.cemconres.2015.05.018.
[11] C01 Committee, C150/C150M − 22, Specification for Portland Cement, ASTM International, n.d. https://doi.org/10.1520/C0150_C0150M-22.
[12] J.F. Young, Portland cements, in: K.H.J. Buschow, R.W. Cahn, M.C. Flemings, B. Ilschner, E.J. Kramer, S. Mahajan, P. Veyssière (Eds.), Encyclopedia of Materials: Science and Technology, Elsevier, Oxford, 2001, pp. 7768–7773, https://doi.org/10.1016/B0-08-043152-6/01398-X.
[13] A. Cuesta, A. Ayuela, M.A.G. Aranda, Belite cements and their activation, Cement Concr. Res. 140 (2021) 106319, https://doi.org/10.1016/j.cemconres.2020.106319.
[14] L. Wang, H.Q. Yang, S.H. Zhou, E. Chen, S.W. Tang, Mechanical properties, long-term hydration heat, shinkage behavior and crack resistance of dam concrete designed with low heat Portland (LHP) cement and fly ash, Construct. Build. Mater. 187 (2018) 1073–1091, https://doi.org/10.1016/j.conbuildmat.2018.08.056.
[15] H.F.W. Taylor, Cement Chemistry 1997, second ed., T. Telford, London, 1997 https://doi.org/10.1680/cc.25929.
[16] F.M. Lea, P.C. Hewlett, M. Liska, Lea's Chemistry of Cement and Concrete, fifth ed., Butterworth-Heinemann, Oxford [England] ; Cambridge, MA, 2019.
[17] R.H. Bogue, Calculation of the compounds in Portland cement, industrial and engineering chemistry, Analytical Edition 1 (1929) 192–197, https://doi.org/10.1021/ac50068a006.
[18] H.F.W. Taylor, Modification of the bogue calculation, Adv. Cement Res. 2 (1989) 73–77, https://doi.org/10.1680/adcr.1989.2.6.73.
[19] T.I. Barry, F.P. Glasser, Calculations of Portland cement clinkering reactions, Adv. Cement Res. 12 (2000) 19–28, https://doi.org/10.1680/adcr.2000.12.1.19.
[20] B. Hökfors, D. Boström, E. Viggh, R. Backman, On the phase chemistry of Portland cement clinker, Adv. Cement Res. 27 (2015) 50–60, https://doi.org/10.1680/adcr.13.00071.
[21] D. Ariño Montoya, N. Pistofidis, G. Giannakopoulos, R.I. Iacobescu, M.S. Katsiotis, Y. Pontikes, Revisiting the iron-rich "ordinary Portland cement" towards valorisation of wastes: study of Fe-to-Al ratio on the clinker production and the hydration reaction, Mater. Struct. 54 (2021) 30, https://doi.org/10.1617/s11527-020-01601-w.
[22] T. Hertel, A. Van den Bulck, S. Onisei, P.P. Sivakumar, Y. Pontikes, Boosting the use of bauxite residue (red mud) in cement - production of an Fe-rich calciumsulfoaluminate-ferrite clinker and characterisation of the hydration, Cement Concr. Res. 145 (2021) 106463, https://doi.org/10.1016/j.cemconres.2021.106463.
[23] A.R.D. Costa, M.V. Coppe, W.V. Bielefeldt, S.A. Bernal, L. Black, A.P. Kirchheim, J. P. Gonçalves, Thermodynamic modelling of cements clinkering process as a tool for optimising the proportioning of raw meals containing alternative materials, Sci. Rep. 13 (2023) 17589, https://doi.org/10.1038/s41598-023-44078-7.
[24] J. Duan, P.G. Asteris, H. Nguyen, X.-N. Bui, H. Moayedi, A novel artificial intelligence technique to predict compressive strength of recycled aggregate concrete using ICA-XGBoost model, Eng. Comput. (2020), https://doi.org/10.1007/s00366-020-01003-0.
[25] A. Behnood, V. Behnood, M.M. Gharehveran, K.E. Alyamac, Prediction of the compressive strength of normal and high-performance concretes using M5P model tree algorithm, Construct. Build. Mater. 142 (2017) 199–207, https://doi.org/10.1016/j.conbuildmat.2017.03.061.
[26] R. Cook, J. Lapeyre, H. Ma, A. Kumar, Prediction of compressive strength of concrete: a critical comparison of performance of a hybrid machine learning model with standalone models, ASCE Journal of Materials in Civil Engineering 31 (2019) 04019255, https://doi.org/10.1061/(ASCE)MT.1943-5533.0002902.
[27] H. Nguyen, T. Vu, T.P. Vo, H.-T. Thai, Efficient machine learning models for prediction of concrete strengths, Construct. Build. Mater. 266 (2021) 120950, https://doi.org/10.1016/j.conbuildmat.2020.120950.
[28] D. Nasr, B. Behforouz, P.R. Borujeni, S.A. Borujeni, B. Zehtab, Effect of nano-silica on mechanical properties and durability of self-compacting mortar containing natural zeolite: experimental investigations and artificial neural network modeling, Construct. Build. Mater. 229 (2019) 116888, https://doi.org/10.1016/j.conbuildmat.2019.116888.
[29] J. Xu, Y. Chen, T. Xie, X. Zhao, B. Xiong, Z. Chen, Prediction of triaxial behavior of recycled aggregate concrete using multivariable regression and artificial neural network techniques, Construct. Build. Mater. 226 (2019) 534–554, https://doi.org/10.1016/j.conbuildmat.2019.07.155.
[30] A. Behnood, E.M. Golafshani, Machine learning study of the mechanical properties of concretes containing waste foundry sand, Construct. Build. Mater. 243 (2020) 118152, https://doi.org/10.1016/j.conbuildmat.2020.118152.
[31] T. Han, A. Siddique, K. Khayat, J. Huang, A. Kumar, An ensemble machine learning approach for prediction and optimization of modulus of elasticity of recycled aggregate concrete, Construct. Build. Mater. 244 (2020) 118271, https://doi.org/10.1016/j.conbuildmat.2020.118271.
[32] Z. Tariq, M. Murtaza, M. Mahmoud, Development of new rheological models for class G cement with nanoclay as an additive using machine learning techniques, ACS Omega 5 (2020) 17646–17657, https://doi.org/10.1021/acsomega.0c02122.
[33] S. Nazar, J. Yang, A. Ahmad, S.F.A. Shah, Comparative study of evolutionary artificial intelligence approaches to predict the rheological properties of fresh concrete, Mater. Today Commun. 32 (2022) 103964, https://doi.org/10.1016/j.mtcomm.2022.103964.
[34] T. Han, R. Bhat, S.A. Ponduru, A. Sarkar, J. Huang, G. Sant, H. Ma, N. Neithalath, A. Kumar, Deep learning to predict the hydration and performance of fly ash-containing cementitious binders, Cement Concr. Res. 165 (2023) 107093, https://doi.org/10.1016/j.cemconres.2023.107093.
[35] T. Han, S.A. Ponduru, R. Cook, J. Huang, G. Sant, A. Kumar, A deep learning approach to design and discover sustainable cementitious binders: strategies to learn from small databases and develop closed-form analytical models, Frontiers in Materials 8 (2022) 796476, https://doi.org/10.3389/fmats.2021.796476.
[36] J. Lapeyre, T. Han, B. Wiles, H. Ma, J. Huang, G. Sant, A. Kumar, Machine learning enables prompt prediction of hydration kinetics of multicomponent cementitious systems, Sci. Rep. 11 (2021) 3922, https://doi.org/10.1038/s41598-021-83582-6.
[37] R. Cook, T. Han, A. Childers, C. Ryckman, K. Khayat, H. Ma, J. Huang, A. Kumar, Machine learning for high-fidelity prediction of cement hydration kinetics in blended systems, Mater. Des. 208 (2021) 109920, https://doi.org/10.1016/j.matdes.2021.109920.
[38] A.M. Ali, J.D. Tabares, M.W. McGinley, A machine learning approach for clinker quality prediction and nonlinear model predictive control design for a rotary cement kiln, Journal of Advanced Manufacturing and Processing 4 (2022) e10137, https://doi.org/10.1002/amp2.10137.
[39] C.W. Bale, E. Bélisle, P. Chartrand, S.A. Decterov, G. Eriksson, A.E. Gheribi, K. Hack, I.-H. Jung, Y.-B. Kang, J. Melançon, A.D. Pelton, S. Petersen, C. Robelin, J. Sangster, P. Spencer, M.-A. Van Ende, FactSage thermochemical software and databases, 2010–2016, Calphad 54 (2016) 35–53, https://doi.org/10.1016/j.calphad.2016.05.002.
[40] F. Kleiner, M. Decker, C. Rößler, H. Hilbig, H.-M. Ludwig, Combined LA-ICP-MS and SEM-EDX analyses for spatially resolved major, minor and trace element detection in cement clinker phases, Cement Concr. Res. 159 (2022) 106875, https://doi.org/10.1016/j.cemconres.2022.106875.
[41] K. Morsli, Á.G. De La Torre, S. Stöber, A.J.M. Cuberos, M. Zahir, M.A.G. Aranda, Quantitative phase analysis of laboratory-active belite clinkers by synchrotron powder diffraction, J. Am. Ceram. Soc. 90 (2007) 3205–3212, https://doi.org/10.1111/j.1551-2916.2007.01870.x.
[42] L. Kacimi, A. Simon-Masseron, S. Salem, A. Ghomari, Z. Derriche, Synthesis of belite cement clinker of high hydraulic reactivity, Cement Concr. Res. 39 (2009) 559–565, https://doi.org/10.1016/j.cemconres.2009.02.004.
[43] T. Hanein, F.P. Glasser, M.N. Bannerman, Thermodynamic data for cement clinkering, Cement Concr. Res. 132 (2020) 106043, https://doi.org/10.1016/j.cemconres.2020.106043.
[44] B. Hökfors, M. Eriksson, E. Viggh, Modelling the cement process and cement clinker quality, Adv. Cement Res. 26 (2014) 311–318, https://doi.org/10.1680/adcr.13.00050.
[45] G. Hou, J. Chen, B. Lu, S. Chen, E. Cui, H.M. Naguib, M.-Z. Guo, Q. Zhang, Composition design and pilot study of an advanced energy-saving and low-carbon rankinite clinker, Cement Concr. Res. 127 (2020) 105926, https://doi.org/10.1016/j.cemconres.2019.105926.

[46] M. Antunes, R.L. Santos, J. Pereira, P. Rocha, R.B. Horta, R. Colaço, Alternative clinker technologies for reducing carbon emissions in cement industry: a critical review, Materials 15 (2022) 209, https://doi.org/10.3390/ma15010209.
[47] R.J. Schalkoff, Artificial Neural Networks, McGraw-Hill, New York, 1997.
[48] M.W. Gardner, S.R. Dorling, Artificial neural networks (the multilayer perceptron)—a review of applications in the atmospheric sciences, Atmos. Environ. 32 (1998) 2627–2636, https://doi.org/10.1016/S1352-2310(97)00447-0.
[49] C. Schaffer, Selecting a classification method by cross-validation, Mach. Learn. 13 (1993) 135–143, https://doi.org/10.1007/BF00993106.
[50] T. Han, N. Stone-Weiss, J. Huang, A. Goel, A. Kumar, Machine learning as a tool to design glasses with controlled dissolution for application in healthcare industry, Acta Biomater. 107 (2020) 286–298, https://doi.org/10.1016/j.actbio.2020.02.037.
[51] R. Cai, T. Han, W. Liao, J. Huang, D. Li, A. Kumar, H. Ma, Prediction of surface chloride concentration of marine concrete using ensemble machine learning, Cement Concr. Res. 136 (2020) 106164, https://doi.org/10.1016/j.cemconres.2020.106164.
[52] A.R.D. Costa, L.B. de B. Barbosa, B.S.R. Kirchheim Ana Paula, J.P. Gonçalves, Thermodynamic Modelling of Belite Clinker Mineralogy during Manufacture, 2023, https://doi.org/10.11159/mmme23.115.
[53] P.E. Stutzman, G. Lespinasse, S.D. Leigh, Compositional Analysis of NIST Reference Material Clinker 8486, NIST, 2000, pp. 22–38.
[54] W. Kurdowski, S. Duszak, B. Trybalska, Belite produced by means of low-temperature synthesis, Cement Concr. Res. 27 (1997) 51–62, https://doi.org/10.1016/S0008-8846(96)00198-6.
[55] C.D. Popescu, M. Muntean, J.H. Sharp, Industrial trial production of low energy belite cement, Cement Concr. Compos. 25 (2003) 689–693, https://doi.org/10.1016/S0958-9465(02)00097-5.
[56] J.H. Sharp, C.D. Lawrence, R. Yang, Calcium sulfoaluminate cements—low-energy cements, special cements or what? Adv. Cement Res. 11 (1999) 3–13, https://doi.org/10.1680/adcr.1999.11.1.3.
[57] A.K. Chatterjee, High belite cements—present status and future technological options: Part I, Cement Concr. Res. 26 (1996) 1213–1225, https://doi.org/10.1016/0008-8846(96)00099-3.
[58] C. Redondo-Soto, D. Gastaldi, S. Irico, F. Canonico, M.A.G. Aranda, Belite clinkers with increasing aluminium content: effect of calcium aluminates on calcium silicate hydration, Cement Concr. Res. 162 (2022) 107015, https://doi.org/10.1016/j.cemconres.2022.107015.
[59] P. Cunningham, J. Carney, S. Jacob, Stability problems with artificial neural networks and the ensemble solution, Artif. Intell. Med. 20 (2000) 217–225, https://doi.org/10.1016/S0933-3657(00)00065-8.
[60] X. Yao, Evolving artificial neural networks, Proc. IEEE 87 (1999) 1423–1447, https://doi.org/10.1109/5.784219.
[61] G. Zhang, B.E. Patuwo, M.Y. Hu, Forecasting with artificial neural networks:: the state of the art, Int. J. Forecast. 14 (1998) 35–62, https://doi.org/10.1016/S0169-2070(97)00044-7.
[62] E. Gomaa, T. Han, M. ElGawady, J. Huang, A. Kumar, Machine learning to predict properties of fresh and hardened alkali-activated concrete, Cement Concr. Compos. 115 (2021) 103863, https://doi.org/10.1016/j.cemconcomp.2020.103863.
[63] B. Lothenbach, K. Scrivener, R.D. Hooton, Supplementary cementitious materials, Cement Concr. Res. 41 (2011) 1244–1256, https://doi.org/10.1016/j.cemconres.2010.12.001.
[64] M. Pelikan, Hierarchical bayesian optimization algorithm, in: M. Pelikan (Ed.), Hierarchical Bayesian Optimization Algorithm: toward a New Generation of Evolutionary Algorithms, Springer Berlin Heidelberg, Berlin, Heidelberg, 2005, pp. 105–129, https://doi.org/10.1007/978-3-540-32373-0_6.
[65] K. Swersky, J. Snoek, R.P. Adams, Multi-task bayesian optimization, in: C.J. C. Burges, L. Bottou, M. Welling, Z. Ghahramani, K.Q. Weinberger (Eds.), Advances in Neural Information Processing Systems, 26, Curran Associates, Inc., 2013, pp. 2004–2012. http://papers.nips.cc/paper/5086-multi-task-bayesian-optimization.pdf. (Accessed 19 June 2018).